

Nonchelated Zr^{IV}–Alkoxide–Alkyne Complexes

Edward J. Stobenau, III and Richard F. Jordan*

Department of Chemistry, The University of Chicago, 5735 South Ellis Avenue, Chicago, Illinois 60637

Received November 3, 2005

Addition of alkynes to [Cp'Zr(O'Bu)][B(C₆F₅)₄] (Cp' = C₅H₄Me, **2**) at low temperature in CD₂Cl₂ solution yields equilibrium mixtures of Cp'Zr(O'Bu)(RC≡CR)⁺ (**3a–g**), **2**, and free alkyne. The ¹³C NMR C_{int} resonance of terminal alkynes shifts far downfield upon coordination, while the C_{term} resonance shifts upfield, consistent with polarization of the C≡C bond with partial positive charge on C_{int} and partial negative charge on C_{term}, probably due to unsymmetrical coordination. Alkynes bind more strongly to **2** than do similar alkenes, but are readily displaced by Lewis bases such as THF. Increasing the steric bulk of the alkyne decreases the coordination strength. Propargyltrimethylsilane coordinates particularly strongly, due to β-Si stabilization of the positive charge on C_{int} of the coordinated alkyne. Compounds **3a–g** undergo two dynamic processes: reversible alkyne decomplexation and rotation around the metal–(alkyne centroid) axis.

Introduction

Alkyne complexes of d⁰ metals are proposed intermediates in alkyne dimerization and oligomerization reactions (Scheme 1)¹ and are potential models for the d⁰ metal–alkene complexes that are intermediates in alkene polymerization.² d⁰ metal–alkyne complexes are challenging to study because alkyne coordination is weak due to the absence of d–π* back-bonding, and facile alkyne insertion can occur if M–H, M–R, or other reactive groups are present. These properties limit the range of ancillary ligands, solvents, and counterions that may be used with these species.

Alkyne complexes of d⁰ metals are very rare. Erker prepared chelated Cp₂M(CMe=C{B(C₆F₅)₃}C≡CMe) (M = Zr, Hf) alkenyl–alkyne complexes (**A**, Chart 1) by the reaction of Cp₂M(C≡CMe)₂ with B(C₆F₅)₃.³ Horton prepared Cp*₂Zr(CH=CRC≡CR)⁺ species (**B**, Cp* = C₅Me₅), which are intermediates in Zr-catalyzed alkyne oligomerization, by insertion of alkynes into Zr–alkynyl compounds.^{1a} Jordan reported similar (η⁵-C₂B₉H₁₁)(Cp*)Hf(CH=CRC≡CR) compounds (**C**), which were generated by analogous reactions.^{1c}

* To whom correspondence should be addressed. E-mail: rfjordan@uchicago.edu.

(1) (a) Horton, A. D. *Chem. Commun.* **1992**, 185. (b) Akita, M.; Yasuda, H.; Nakamura, A. *Bull. Chem. Soc. Jpn.* **1984**, 57, 480. (c) den Haan, K. H.; Wielstra, Y.; Teuben, J. H. *Organometallics* **1987**, 6, 2053. (d) Heeres, H. J.; Teuben, J. H. *Organometallics* **1991**, 10, 1980. (e) Yoshida, M.; Jordan, R. F. *Organometallics* **1997**, 16, 4508. (f) Nishiura, M.; Hou, Z. *J. Mol. Catal. A: Chem.* **2004**, 213, 101. (g) Mach, K.; Gyepes, R.; Horáček, M.; Petrusová, L.; Kubišta, J. *Collect. Czech. Chem. Commun.* **2003**, 68, 1877. (h) Varga, V.; Petrusová, L.; Čejka, J.; Hanuš, V.; Mach, K. *J. Organomet. Chem.* **1996**, 509, 235. (i) Ohff, A.; Burlakov, V. V.; Rosenthal, U. *J. Mol. Catal. A: Chem.* **1996**, 108, 119.

(2) For recent review articles concerning metal-catalyzed alkene polymerization see: (a) Mülhaupt, R. *Macromol. Chem. Phys.* **2003**, 204, 289. (b) Resconi, L.; Cavallo, L.; Fait, A.; Piemontesi, F. *Chem. Rev.* **2000**, 100, 1253. (c) Brintzinger, H. H.; Fischer, D.; Mülhaupt, R.; Rieger, B.; Waymouth, R. M. *Angew. Chem., Int. Ed. Engl.* **1995**, 34, 1143.

(3) (a) Temme, B.; Erker, G.; Fröhlich, R.; Grehl, M. *Angew. Chem., Int. Ed. Engl.* **1994**, 33, 1480. (b) Venne-Dunker, S.; Ahlers, W.; Erker, G.; Fröhlich, R. *Eur. J. Inorg. Chem.* **2000**, 1671. (c) Ahlers, W.; Erker, G.; Fröhlich, R.; Peuchert, U. *J. Organomet. Chem.* **1999**, 578, 115. (d) Ahlers, W.; Temme, B.; Erker, G.; Fröhlich, R.; Fox, T. *J. Organomet. Chem.* **1997**, 527, 191. (e) Erker, G.; Venne-Dunker, S.; Kehr, G.; Kleigrew, N.; Fröhlich, R.; Mück-Lichtenfeld, C.; Grimme, S. *Organometallics* **2004**, 23, 4391. (f) Burlakov, V. V.; Arndt, P.; Baumann, W.; Spannenberg, A.; Rosenthal, U. *Organometallics* **2004**, 23, 5188.

Scheme 1

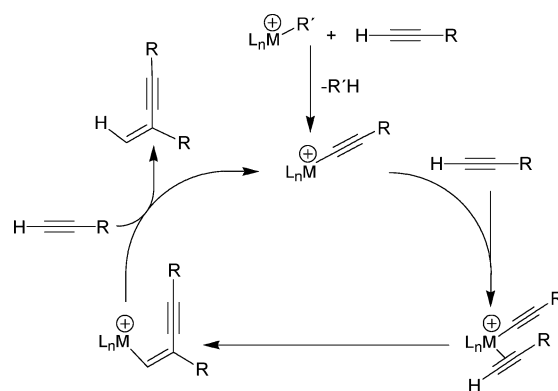
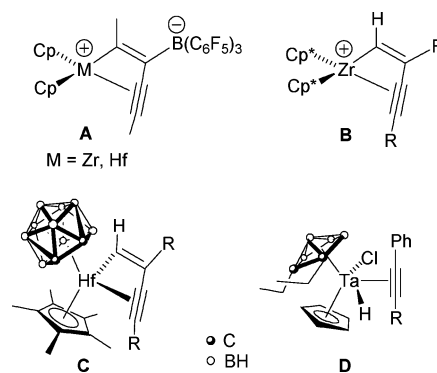


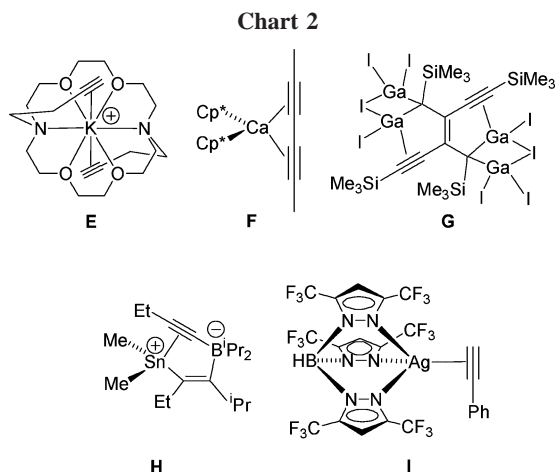
Chart 1



The C≡C NMR resonances of **B** and **C** are 5–10 ppm downfield from the resonances in typical enynes.^{1b} Finn and Grimes reported that the reaction of { (η⁵-Et₂C₂B₄H₄)CpTaH }₂-(μ-Cl)₂ with diphenylacetylene or 1-phenylpropyne yields nonchelated alkyne complexes (η⁵-Et₂C₂B₄H₄)CpTa(H)(Cl)-(PhC≡CR) (**D**; R = Ph, Me).⁴ ¹³C NMR chemical shifts for the C≡C carbons in these species were not reported. Theoretical

(4) Curtis, M. A.; Finn, M. G.; Grimes, R. N. *J. Organomet. Chem.* **1998**, 550, 469.

(5) (a) Hyla-Kryspin, I.; Gleiter, R. *J. Mol. Catal. A: Chem.* **2000**, 160, 115. (b) Hyla-Kryspin, I.; Niu, S.; Gleiter, R. *Organometallics* **1995**, 14, 964.



studies of $\text{Cp}_2\text{ZrMe}(\text{HC}\equiv\text{CH})^+$, $\text{Cl}_2\text{ZrH}(\text{HC}\equiv\text{CH})^+$, and $\text{Cl}_2\text{ZrMe}(\text{HC}\equiv\text{CH})^+$ predict an unsymmetrical bonding mode for Zr^{IV} -alkyne complexes.⁵ For example, the $\text{Zr}-\text{C}_{\text{alkyne}}$ distances in $\text{Cp}_2\text{ZrMe}(\text{HC}\equiv\text{CH})^+$ were calculated to be 2.640 and 2.787 Å ($\Delta d(\text{Zr}-\text{C}) = 0.147$ Å).

Alkyne complexes of s- and p-block elements have also been characterized. Gokel reported that crown ethers with tethered alkynes exhibit Na^+ - or K^+ -alkyne interactions in the solid state (**E**, Chart 2),⁶ and Hanusa described the diyne complex $\text{Cp}^*_2\text{Ca}(\text{Me}_3\text{SiC}\equiv\text{CC}\equiv\text{CSiMe}_3)$ (**F**).⁷ The NMR resonances of the alkyne units in these compounds are only slightly shifted from the free alkyne positions.^{6b,7} Jones reported that the reaction of “GaI” with $\text{Me}_3\text{SiC}\equiv\text{CC}\equiv\text{CSiMe}_3$ yields a novel Ga^{III}_4 cluster with two Ga-alkyne units (**G**).⁸ Wrackmeyer has studied $\text{Sn}^{\text{IV}}-\eta^2$ -alkynylborate adducts that are intermediates in stannole formation (e.g., **H**)⁹ and has reported similar $\text{Pb}^{\text{IV}}-\eta^2$ -alkynylborate compounds.¹⁰

Group 11 and 12 metal-alkyne complexes in which $d-\pi^*$ back-bonding is very weak have also been studied. For example, $d^{10}\text{Ag}^{\text{I}}$ compounds normally exhibit only minimal $d-\pi^*$ back-bonding, as exemplified by $(\text{HB}\{(3,5\text{-CF}_3)_2\text{pz}\}_3)\text{Ag}(\text{CO})$, for which a very high ν_{CO} value (2162 cm^{-1}) was observed.¹¹ Dias prepared Ag^{I} -alkyne adducts such as $(\text{HB}\{(3,5\text{-CF}_3)_2\text{pz}\}_3)\text{Ag}(\text{HC}\equiv\text{CPh})$ (**I**; pz = pyrazolyl).¹¹ Compound **I** exhibits unsymmetrical Ag-alkyne bonding in the solid state ($d(\text{Ag}-\text{C}_{\text{term}}) = 2.263(5)$ Å; $d(\text{Ag}-\text{C}_{\text{int}}) = 2.407(5)$ Å; $\Delta d(\text{Ag}-\text{C}) = d(\text{Ag}-\text{C}_{\text{int}}) - d(\text{Ag}-\text{C}_{\text{term}}) = 0.144(7)$ Å). The coordination shifts ($\Delta\delta = \delta_{\text{coord}} - \delta_{\text{free}}$) of the alkyne $\text{C}\equiv\text{C}$ NMR resonances of **I** are opposite in sign ($\Delta\delta\text{C}_{\text{term}} = -11.1$; $\Delta\delta\text{C}_{\text{int}} = 2.8$), which may be a consequence of the unsymmetrical coordination. Other Ag^{I} alkyne adducts have been reported.¹² Starowieyski has studied ω -alkynyl zinc compounds that have chelated structures with alkyne-zinc interactions.¹³

(6) (a) Hu, J.; Barbour, L. J.; Gokel, G. W. *J. Am. Chem. Soc.* **2001**, *123*, 9486. (b) Hu, J.; Gokel, G. W. *Chem. Commun.* **2003**, 2536.

(7) Williams, R. A.; Hanusa, T. P.; Huffman, J. C. *J. Am. Chem. Soc.* **1990**, *112*, 2454.

(8) Baker, R. J.; Jones, C. *Chem. Commun.* **2003**, 390.

(9) (a) Wrackmeyer, B.; Kehr, G.; Willbold, S. *J. Organomet. Chem.* **1999**, *590*, 93. (b) Wrackmeyer, B.; Vollrath, H.; Ali, S. *Inorg. Chim. Acta* **1999**, *296*, 26. (c) Wrackmeyer, B.; Horchler von Locquenghien, K.; Kundler, S. *J. Organomet. Chem.* **1995**, *503*, 289. (d) Wrackmeyer, B.; Kehr, G.; Wettinger, D. *Inorg. Chim. Acta* **1994**, *220*, 161. (e) Wrackmeyer, B.; Kehr, G.; Boese, R. *Angew. Chem., Int. Ed. Engl.* **1991**, *30*, 1370. (f) Wrackmeyer, B.; Kundler, S.; Milius, W.; Boese, R. *Chem. Ber.* **1994**, *127*, 333. (g) Wrackmeyer, B.; Kundler, S.; Boese, R. *Chem. Ber.* **1993**, *126*, 1361. (h) Wrackmeyer, B.; Kehr, G.; Sebald, A.; Kümmerlen, J. *Chem. Ber.* **1992**, *125*, 1597.

(10) (a) Wrackmeyer, B.; Horchler, K. *J. Organomet. Chem.* **1990**, *399*, 1. (b) Wrackmeyer, B.; Horchler, K.; Boese, R. *Angew. Chem., Int. Ed. Engl.* **1989**, *28*, 1500.

(11) Dias, H. V. R.; Wang, Z.; Jin, W. *Inorg. Chem.* **1997**, *36*, 6205.

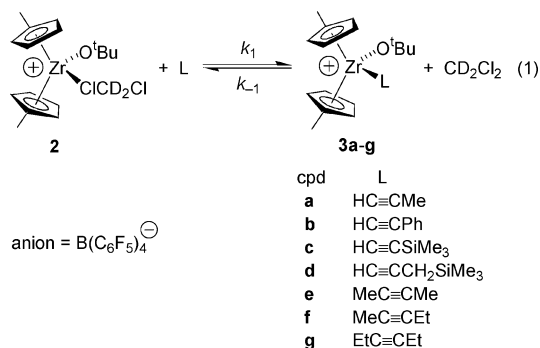
This paper describes the synthesis and properties of nonchelated $\text{Cp}'_2\text{Zr}(\text{O}^t\text{Bu})(\text{alkyne})^+$ ($\text{Cp}' = \text{C}_5\text{H}_4\text{Me}$) complexes, which are models for the putative $(\text{C}_5\text{R}_5)_2\text{Zr}(\text{R}')(\text{alkyne})^+$ intermediates in Zr-catalyzed alkyne oligomerization reactions.¹⁴

Results and Discussion

Targets. The objective of this work was to prepare $[\text{Cp}'_2\text{Zr}(\text{O}^t\text{Bu})(\text{RC}\equiv\text{CR}')][\text{B}(\text{C}_6\text{F}_5)_4]$ alkyne complexes in order to probe Zr^{IV} -alkyne bonding. The *tert*-butoxide ligand was used to generate an electrophilic three-coordinate Zr species that cannot undergo alkyne insertion due to the strong Zr-O bond.¹⁵ The Cp' ligand was chosen because it provides a useful symmetry probe and neutral precursors to $\text{Cp}'_2\text{Zr}(\text{OR})^+$ are readily available. The $\text{B}(\text{C}_6\text{F}_5)_4^-$ anion was chosen for its high stability and weak coordinating ability.¹⁶ Halocarbon solvents were used to solubilize the ionic species, albeit at the cost of competitive solvent coordination.¹⁷

Synthesis of $[\text{Cp}'_2\text{Zr}(\text{O}^t\text{Bu})][\text{B}(\text{C}_6\text{F}_5)_4]$. The reaction of $\text{Cp}'_2\text{ZrMe}_2$ with $^t\text{BuOH}$ yields $\text{Cp}'_2\text{Zr}(\text{O}^t\text{Bu})\text{Me}$ (**1**).¹⁸ The reaction of **1** with $[\text{Ph}_3\text{C}][\text{B}(\text{C}_6\text{F}_5)_4]$ affords $[\text{Cp}'_2\text{Zr}(\text{O}^t\text{Bu})][\text{B}(\text{C}_6\text{F}_5)_4]$ (**2**).^{14a}

Generation of $\text{Cp}'_2\text{Zr}(\text{O}^t\text{Bu})(\text{alkyne})^+$ Complexes. Addition of excess alkyne to a CD_2Cl_2 solution of **2** at low temperature results in the formation of an equilibrium mixture of **2**, free alkyne, and $[\text{Cp}'_2\text{Zr}(\text{O}^t\text{Bu})(\text{alkyne})][\text{B}(\text{C}_6\text{F}_5)_4]$ (**3a-g**), as shown in eq 1. In a typical experiment, the desired alkyne was added by vacuum transfer to a frozen solution of **2** in CD_2Cl_2 in an NMR tube. The tube was thawed, stored at -78 °C, and transferred to a precooled NMR probe with minimal transfer time (<1 min) to prevent side reactions, and the equilibrium in eq 1 was studied by NMR spectroscopy. The $\text{Cp}'_2\text{Zr}(\text{O}^t\text{Bu})(\text{alkyne})^+$ species are thermally sensitive, which precluded isolation or ESI-MS analysis.



NMR Properties and Solution Structures of $\text{Cp}'_2\text{Zr}(\text{O}^t\text{Bu})(\text{alkyne})^+$ Complexes.

The ^1H and $^{13}\text{C}\{^1\text{H}\}$ NMR spectra of (12) (a) Ginnebaugh, J. P.; Maki, J. W.; Lewandos, G. S. *J. Organomet. Chem.* **1980**, *190*, 403. (b) Schulte, P.; Behrens, U. *J. Organomet. Chem.* **1998**, *563*, 235. (c) Chi, K.-M.; Lin, C.-T.; Peng, S.-M.; Lee, G.-H. *Organometallics* **1996**, *15*, 2660. (d) Gleiter, R.; Karcher, M.; Kratz, D.; Ziegler, M. L.; Nuber, B. *Chem. Ber.* **1990**, *123*, 1461.

(13) Oknińska, E.; Starowieyski, K. B. *J. Organomet. Chem.* **1989**, *376*, 7.

(14) Preliminary communications: (a) Stoebenau, E. J., III; Jordan, R. F. *J. Am. Chem. Soc.* **2003**, *125*, 3222. (b) Stoebenau, E. J., III; Jordan, R. F. *J. Am. Chem. Soc.* **2004**, *126*, 11170.

(15) (a) Lappert, M. F.; Patil, D. S.; Pedley, J. B. *Chem. Commun.* **1975**, 830. (b) Schock, L. E.; Marks, T. J. *J. Am. Chem. Soc.* **1988**, *110*, 7701.

(16) (a) Krossing, I.; Raabe, I. *Angew. Chem., Int. Ed.* **2004**, *43*, 2066. (b) Strauss, S. H. *Chem. Rev.* **1993**, *93*, 927. (c) Chen, E. Y.-X.; Marks, T. J. *Chem. Rev.* **2000**, *100*, 1391. (d) Massey, A. G.; Park, A. J. *J. Organomet. Chem.* **1964**, *1*, 245. (e) Chien, J. C. W.; Tsai, W.-M.; Rausch, M. D. *J. Am. Chem. Soc.* **1991**, *113*, 8570. (f) Turner, H. W. Eur. Patent EP0277004, 1988.

Table 1. NMR Coordination Shifts ($\Delta\delta$) for Cp'₂Zr(O^tBu)(HC≡CR)⁺ Complexes (**3a–d**)^a

cpd	alkyne	C _{int}	C _{term}	C _{prop} ^b	H _{term}	H _{prop} ^b
3a	HC≡CMe	8.9	-2.8	4.5	1.16	0.46
3b	HC≡CPh	13.3	-2.1		1.23	
3c	HC≡CSiMe ₃	4.8	-2.9		0.98	
3d	HC≡CCH ₂ SiMe ₃	21.7	-0.9	7.0	1.58	0.48

^a In CD₂Cl₂ solution, -89 °C; $\Delta\delta = \delta_{\text{coord}} - \delta_{\text{free}}$. ^b HC≡CCH_nR_{3-n} resonance.

3a–g each contain four CH resonances and one set of CMe resonances for the Cp' ligands, and one set of O^tBu resonances, characteristic of C_s symmetry. In most cases, the Cp' resonances are only slightly shifted from those of **2**. The Zr–O^tBu ¹H NMR resonance appears at δ 1.22 for **2** and shifts less than 0.05 ppm from this position for **3a,c–g**. However, the Zr–O^tBu ¹H NMR resonance of the phenylacetylene adduct **3b** is shifted upfield to δ 0.80, which is ascribed to anisotropic shielding of the O^t-Bu hydrogens by the phenyl ring of the coordinated alkyne.

The NMR spectra of terminal alkyne complexes **3a–d** each contain one set of alkyne resonances, which are shifted from the free alkyne positions. The C_s symmetry and the presence of only one set of alkyne signals are consistent with the presence of a single rotamer of **3a–d** in which the alkyne lies in the plane between the Cp' ligands or with fast rotation around the Zr–(alkyne centroid) axis.

The NMR spectra of symmetrical-alkyne adducts **3e,g** each contain one set of alkyne ≡CR resonances. The C_s symmetry of **3e,g** and the presence of only one set of ≡CR signals are consistent with the presence of a single rotamer of **3e,g** in which the alkyne lies perpendicular to the plane between the Cp' ligands or with fast rotation around the Zr–(alkyne centroid) axis. The 2-butyne ¹H and ¹³C NMR resonances of **3e** have approximately the same line widths as the other signals of **3e** at -59 °C, where intermolecular alkyne exchange is slow on the NMR time scale, but broaden as the temperature is lowered to -89 °C, while the other resonances of **3e** remain sharp. Similar NMR line-broadening effects are observed for the 2-pentyne (**3f**) and 3-hexyne (**3g**) adducts. These results indicate that rotation around the metal–(alkyne centroid) axis is fast on the NMR time scale at higher temperatures, but decreases in rate at lower temperatures.

The alkyne NMR resonances of the terminal alkyne complexes **3a–d** exhibit characteristic coordination shifts ($\Delta\delta = \delta_{\text{coord}} - \delta_{\text{free}}$), which are listed in Table 1. The HC≡ (C_{term}) ¹³C resonance shifts upfield by 1–3 ppm, while the ≡CR (C_{int}) resonance shifts significantly downfield ($\Delta\delta = 5–22$) upon coordination. The alkyne region of the ¹³C{¹H} NMR spectrum of **3a** is shown in Figure 1 and illustrates the divergent coordination shifts of the MeC≡CH resonances. The ≡CH (H_{term}) ¹H NMR resonance of **3a–d** shifts downfield by 1–2

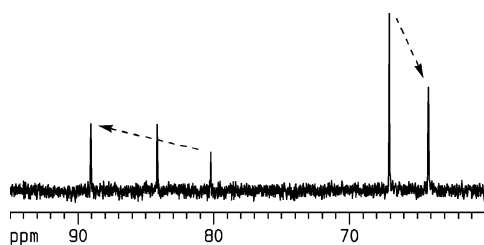


Figure 1. Partial ¹³C{¹H} NMR spectrum of **3a** (CD₂Cl₂, -89 °C). Assignments: δ 89 (C_{int} of **3a**), 84 (OCMe₃ of **2** and **3a**), 80 (C_{int} of free propyne), 67 (C_{term} of free propyne), 64 (C_{term} of **3a**). The coordination shifts (free to coordinated) for the alkyne resonances are shown by arrows.

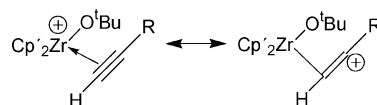


Figure 2. Polarization of d⁰ metal–alkyne complexes.

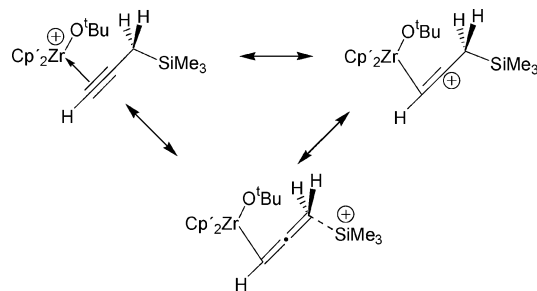


Figure 3. Stabilization of propargyltrimethylsilane adduct **3d** by the β -Si effect.

ppm upon coordination. For **3a,d**, the propargylic ≡CCH_n ¹H and ¹³C resonances are shifted downfield by ca. 0.5 and 5–7 ppm, respectively.

The ¹³C $\Delta\delta$ values are reminiscent of the divergent coordination shifts in chelated (C₅R₅)₂Zr(OCMe₂CH₂CH₂CH=CH₂)⁺ complexes¹⁹ and the Ag^I(HC≡CPh) adduct **I**,¹¹ for which X-ray crystallographic analyses establish that the alkene and alkyne ligands are unsymmetrically bound. Therefore, the alkyne ligands in **3a–d** are also probably unsymmetrically coordinated with $d(\text{Zr}-\text{C}_{\text{int}}) > d(\text{Zr}-\text{C}_{\text{term}})$. Unsymmetrical alkyne coordination will polarize the C≡C triple bond, resulting in positive charge buildup on C_{int} and negative charge buildup on C_{term} (Figure 2), which explains the NMR data in Table 1. Consistent with this picture, propargyltrimethylsilane complex **3d** exhibits the largest $\Delta\delta$ value for C_{int}, which is a consequence of β -Si stabilization of the positive charge on C_{int}, as shown in Figure 3.^{20,21} In contrast, the trimethylsilylacetylene adduct **3c** exhibits the smallest $\Delta\delta$ value for C_{int}, because the α -Si is better at stabilizing an anionic charge than a positive charge at C_{int}, resulting in reduced alkyne polarization.

The ¹J_{CH} and ²J_{C=CH} coupling constants for the alkyne units in **3a–d** are only slightly perturbed from the free alkyne values, as summarized in Table 2. These results suggest that the alkyne structure and the hybridization at the alkyne carbons are not strongly perturbed by coordination.

The coordination shifts of internal alkyne complexes **3e–g** are listed in Table 3. The C_{alkyne} NMR resonances of **3e–g** shift

(17) (a) Wu, F.; Dash, A. K.; Jordan, R. F. *J. Am. Chem. Soc.* **2004**, *126*, 15360. (b) Bouwkamp, M. W.; Budzelaar, P. H. M.; Gercama, J.; Del Hierro Morales, I.; de Wolf, J.; Meetsma, A.; Troyanov, S. I.; Teuben, J. H.; Hessen, B. *J. Am. Chem. Soc.* **2005**, *127*, 14310. (c) Korolev, A. V.; Delpech, F.; Dagorne, S.; Guzei, I. A.; Jordan, R. F. *Organometallics* **2001**, *20*, 3367.

(18) (a) Brandow, C. G. Zirconocenes as Models for Homogeneous Ziegler–Natta Olefin Polymerization Catalysts. Ph.D. Thesis, California Institute of Technology, Pasadena, CA, 2001. See also: (b) Wailes, P. C.; Weigold, H.; Bell, A. P. *J. Organomet. Chem.* **1972**, *34*, 155. (c) Takahashi, T.; Aoyagi, K.; Hara, R.; Suzuki, N. *Chem. Lett.* **1992**, 1693.

(19) Carpentier, J. F.; Wu, Z.; Lee, C. W.; Strömberg, S.; Christopher, J. N.; Jordan, R. F. *J. Am. Chem. Soc.* **2000**, *122*, 7750.

(20) (a) Lambert, J. B. *Tetrahedron* **1990**, *46*, 2677. (b) Müller, T.; Juhasz, M.; Reed, C. A. *Angew. Chem., Int. Ed.* **2004**, *43*, 1543. (c) Müller, T.; Meyer, R.; Lennartz, D.; Siehl, H.-U. *Angew. Chem., Int. Ed.* **2000**, *39*, 3074. (d) Müller, T.; Margraf, D.; Syha, Y. *J. Am. Chem. Soc.* **2005**, *127*, 10852.

(21) (a) Boag, N. M.; Green, M.; Grove, D. M.; Howard, J. A. K.; Spencer, J. L.; Stone, F. G. A. *J. Chem. Soc., Dalton. Trans.* **1980**, 2170. (b) Bartik, T.; Happ, B.; Iglewsky, M.; Bandmann, H.; Boese, R.; Heimbacht, P.; Hoffmann, T.; Wenschuh, E. *Organometallics* **1992**, *11*, 1235. (c) Rosenthal, U.; Burlakov, V. V.; Arndt, P.; Baumann, W.; Spannenberg, A. *Organometallics* **2003**, *22*, 884, and references therein.

Table 2. Coupling Constants for Free Alkynes and Alkynes Coordinated to 2^a

cpd	alkyne	¹ J _{CH} (Hz)		² J _{C≡CH} (Hz)	
		coord	free	coord	free
3a	HC≡CMe	251	249	47	50
3b	HC≡CPh	246	252	41	50
3c	HC≡CSiMe ₃	244	237	<i>x^b</i>	41
3d	HC≡CCH ₂ SiMe ₃	244	247	43	50

^a In CD₂Cl₂ solution, -89 °C. ^b Determination of this coupling constant was precluded by spectral overlaps.

Table 3. NMR Coordination Shifts (Δδ) for Cp'Zr(O'Bu)(RC≡CR)⁺ Complexes (3e–g)^a

cpd	alkyne	C _{alkyne}	C _{prop^b}	H _{prop^b}
3e	MeC≡CMe	5.4	6.6	0.35
3f	MeC≡CEt	7.3 ^c	6.8 ^c	0.36 ^c
		3.8 ^d	7.2 ^d	<i>x^{d,e}</i>
3g	EtC≡CEt	6.1	7.0	<i>x^e</i>

^a In CD₂Cl₂ solution, -89 °C; Δδ = δ_{coord} - δ_{free}. ^b ≡CCH_nR_{3-n} resonance. ^c MeC≡ resonances. ^d EtC≡ resonances. ^e Resonance not detected due to spectral overlaps.

Table 4. Equilibrium Constants (K_{eq}) for Alkyne Coordination to Cp'Zr(O'Bu)(ClCD₂Cl)⁺ in Eq 1^a

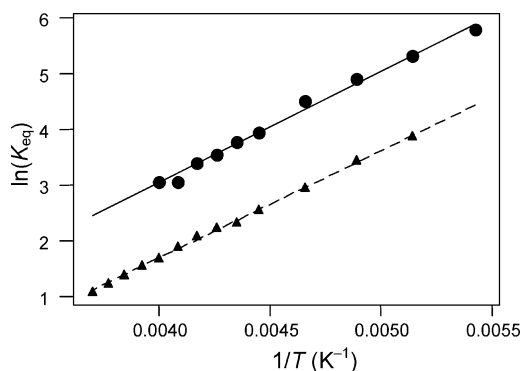
cpd	alkyne	K _{eq} (M ⁻¹) ^b
3d	HC≡CCH ₂ SiMe ₃	1.0(2) × 10 ⁵
3a	HC≡CMe	360(70)
3e	MeC≡CMe	52(3)
3f	MeC≡CEt	49(9)
3g	EtC≡CEt	47(4)
3b	HC≡CPh	22(1)
3c	HC≡CSiMe ₃	8.1(5)
	HC≡C'Bu	<i>x^c</i>

^a In CD₂Cl₂ solution, -89 °C. ^b K_{eq} = [3][2]⁻¹[L]⁻¹. ^c No complex observed; K_{eq} ≤ 0.1 M⁻¹.

downfield by 4–7 ppm and the C_{prop} resonances shift downfield by ca. 7 ppm upon coordination. The H_{prop} resonances also display moderate downfield coordination shifts (Δδ = ca. 0.4 ppm).

The NMR properties of **3e–g** can be rationalized by the unsymmetrical coordination/alkyne polarization model proposed above for terminal alkyne complexes, coupled with fast exchange of the ends of the alkyne by rotation around the metal–(alkyne centroid) axis. Under slow alkyne rotation conditions, one alkyne carbon resonance of an unsymmetrically bound symmetrical alkyne would shift slightly upfield, while the other would shift significantly downfield, as observed for terminal alkyne adducts **3a–d**. Alkyne rotation would average these resonances, resulting in a net downfield shift, as observed for **3e–g**. The proposed unsymmetrical alkyne coordination in **3e–g** is consistent with the computational results for Cp₂ZrMe-(HC≡CH)⁺ noted above.⁵

Oxymetalloacyclobutene-type structures derived from alkyne insertion, i.e., Cp'Zr(κ²-C,O-CR=CRO'Bu)⁺, are ruled out for **3a–g** because such structures would display much larger Δδ values for the alkyne fragment than are observed, analogous to those for azametalloacyclobutene species, i.e., Cp₂Zr(κ²-C,N-CR=CRNR).²²

**Figure 4.** van't Hoff plot for propyne (circles, solid line) and 2-butyne (triangles, dashed line) coordination in **3a,e** in CD₂Cl₂ solution (eq 1).

Thermodynamics of Alkyne Binding to 2. Equilibrium constants for alkyne binding to **2** in eq 1, K_{eq} = [3][2]⁻¹[L]⁻¹, were determined by ¹H NMR and are listed in Table 4.²³ K_{eq} values for **3a–c,e–g** were found by studies of eq 1. The K_{eq} value for propargyltrimethylsilane binding was too large to be determined directly and, therefore, was determined by a competition experiment with propyne. In certain cases, K_{eq} values were determined over a sufficiently wide temperature range to enable accurate determination of binding enthalpies and entropies. These values are listed in Table 5.

The binding of 2-butyne to **2** to form **3e** in eq 1 will be described as a representative case. The equilibrium constant for 2-butyne coordination in CD₂Cl₂ solution at -89 °C is K_{eq} = 52(3) M⁻¹. At [2]_{initial} = 0.08 M and [2-butyne]_{initial} = 0.10 M, ca. 75% of the total Cp'Zr(O'Bu)⁺ exists as **3e**. The K_{eq} value is constant over the concentration ranges [2]_{initial} = 0.035–0.078 M and [2-butyne]_{initial} = 0.043–0.10 M. Addition of [Ph₃C][B(C₆F₅)₄] (ca. 4 equiv per Zr) as an anion source does not affect the equilibrium constant at -91 °C in CD₂Cl₂, indicating that the anion is not explicitly involved in eq 1. Under these conditions, Ph₃C⁺ does not interact with 2-butyne or **2**. At -38 °C, K_{eq} for 2-butyne binding is larger in CD₂Cl₂ (8.8(4) M⁻¹) than in C₆D₅Cl (2.9(1) M⁻¹). While solvent polarity may influence the K_{eq} value,²⁴ it is likely that PhCl binds to **2** more strongly than CD₂Cl₂ does,^{17a} which would result in a reduced K_{eq} value in the former solvent. As the temperature is raised, the 2-butyne complex **3e** becomes less favored, and the equilibrium shifts to free alkyne and **2**. A van't Hoff analysis (Figure 4) gives ΔH° = -3.6(3) kcal/mol and ΔS° = -11(1) eu (Table 5).²³

The data in Table 4 show how the steric and electronic properties of the alkyne influence K_{eq}. Steric crowding close to the alkyne triple bond inhibits alkyne coordination. Propyne binds more strongly than 2-butyne or other internal alkynes, and *tert*-butylacetylene does not bind to **2** in CD₂Cl₂ solution. Propyne coordination is strong enough to observe NMR line broadening in a 2/propyne mixture at 22 °C. Internal alkynes must have one alkyl group in the vicinity of the Cp' rings in the Cp'Zr(O'Bu)(RC≡CR)⁺ adduct, while propyne does not.

Stabilization of the partial positive charge on C_{int} of the coordinated alkyne enhances alkyne binding. Thus, due to the

Table 5. Thermodynamic Data for Equilibria in Eq 1 and Activation Parameters for Decomplexation (k₋₁)^a

cpd	alkyne	ΔH° (kcal/mol)	ΔS° (eu)	ΔH [‡] (kcal/mol)	ΔS [‡] (eu)	ΔG [‡] (kcal/mol) ^b
3a	HC≡CMe	-4.1(3)	-11(1)	8.5(3)	-14(1)	11.8(1)
3e	MeC≡CMe	-3.6(3)	-11(1)	13.8(5)	4(2)	12.9(1)

^a In CD₂Cl₂ solution. ^b At -39 °C.

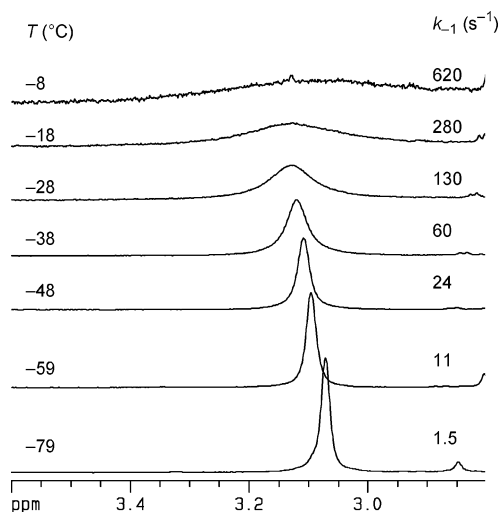


Figure 5. Partial variable-temperature ¹H NMR spectra (500 MHz) of an equilibrium mixture of **3a**, **2**, and propyne in CD₂Cl₂ solution illustrating the broadening of the H_{term} resonance of **3a** (δ 3.1) due to reversible propyne decomplexation. The k_{-1} values are first-order rate constants for propyne decomplexation. The peak at δ 2.85 is due to an unidentified impurity.

operation of the β -Si effect, propargyltrimethylsilane coordinates very strongly to **2** to give **3d** (Table 4), and the presence of just 1 equiv of propargyltrimethylsilane results in quantitative formation of **3d** up to -8 °C.²⁰

The binding enthalpies in Table 5 show that the Zr-alkyne bonds in **3a,e** are only ca. 4 kcal/mol stronger than the Zr-CICD₂Cl bond in **2**, which underscores the point that the absence of d- π^* back-bonding results in weak alkyne coordination. Alkyne binding is substantially weaker than coordination of typical Lewis bases. For example, 1 equiv of THF (per Zr) completely displaces propyne from **3a** to give [Cp'₂Zr(O^tBu)(THF)][B(C₆F₅)₄] (**4**). Compound **4** can be independently generated by addition of THF to a solution of **2**. The properties of **4** are similar to those of Cp₂Zr(O^tBu)(THF)⁺ and *rac*-(EBTHI)Zr(O^tBu)(THF)⁺ (EBTHI = 1,2-ethylenebis(tetrahydroindenyl)).²⁵

Intermolecular Alkyne Exchange. The NMR resonances for **3a**, **2**, and free propyne in an equilibrium mixture of these species broaden as the temperature is raised above -69 °C. The Cp'CH ¹H NMR signals of **3a** coalesce with those of **2** between -38 and -18 °C, and the bound propyne signals of **3a** coalesce with the free propyne signals between -8 and $+22$ °C. These dynamic effects are consistent with the exchange of **3a** and **2** and of free and coordinated propyne. The broadening of the H_{term} resonance of **3a** is shown in Figure 5.

First-order rate constants for propyne decomplexation from **3a** (k_{-1} in eq 1) were determined from the excess line broadening of the H_{term} resonance of **3a** under slow NMR exchange conditions. The line width of the H_{term} resonance and

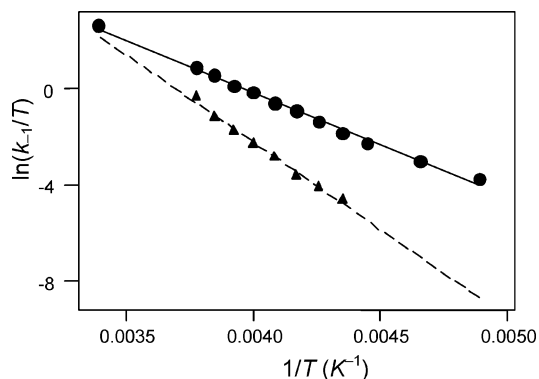
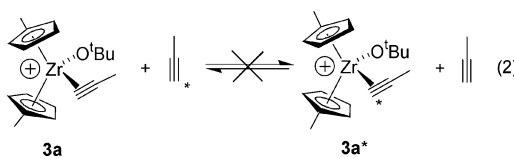


Figure 6. Eyring plot for propyne (circles, solid line) and 2-butyne (triangles, dashed line) decomplexation (k_{-1}) from **3a,e** in CD₂Cl₂ solution.

hence the propyne decomplexation rate constant is independent of the free propyne concentration over the range [propyne] = 0.017–0.048 M. Therefore, direct associative displacement of coordinated propyne by free propyne (eq 2) does not occur to a significant extent. Instead, the data imply that propyne is lost from **3a** to give **2**, and propyne coordinates to **2** to give **3a** (eq 1).



An Eyring analysis (Figure 6) for propyne decomplexation from **3a** gives the activation parameters listed in Table 5. The negative ΔS^\ddagger value suggests that a CD₂Cl₂ molecule displaces the coordinated propyne by an associative mechanism.

Similarly, when a solution of **3e** is warmed above -48 °C, the NMR signals of **3e** broaden and coalesce with the signals for **2** and free 2-butyne. First-order rate constants for 2-butyne decomplexation (k_{-1}) were determined from the excess line broadening of the 2-butyne ¹H NMR resonance of **3e**. The first-order rate constants are independent of the free 2-butyne concentration over the range [MeC≡CMe] = 0.037–0.079 M. Therefore, free 2-butyne does not directly displace coordinated 2-butyne in the exchange process.

An Eyring analysis for 2-butyne decomplexation from **3e** (Figure 6) gives the activation parameters listed in Table 5. The small, positive ΔS^\ddagger value and larger ΔH^\ddagger value compared to that for propyne decomplexation from **3a** are consistent with a greater degree of dissociative character for 2-butyne decomplexation versus propyne decomplexation. Significant steric crowding is expected in the transition state for associative CD₂Cl₂ displacement of 2-butyne from **3e**.

A free energy diagram comparing propyne and 2-butyne coordination to **2** is shown in Figure 7. 2-Butyne binds more weakly, but exchanges more slowly than propyne. These differences reflect the greater steric crowding in the 2-butyne adduct.

Comparison of Properties of d⁰ and d² Group 4 Alkyne Complexes. Due to the absence of d- π^* back-bonding in alkyne adducts **3a–g**, the properties of these compounds are quite different from those of “classical” dⁿ metal-alkyne complexes, in which back-bonding is present. These differences can be illustrated most clearly by comparing d⁰ Zr^{IV}-alkyne adducts to d² Zr^{II}-alkyne adducts. Buchwald studied the hexyne adducts Cp₂Zr(HC≡CⁿBu)(PMe₃) (**J**) and Cp₂Zr(EtC≡CEt)-

(22) (a) Walsh, P. J.; Hollander, F. J.; Bergman, R. G. *Organometallics* **1993**, *12*, 3705. (b) Harlan, C. J.; Tunge, J. A.; Bridgewater, B. M.; Norton, J. R. *Organometallics* **2000**, *19*, 2365.

(23) If the solvent term is included, the equilibrium constant for eq 1 is $K'_{eq} = K_{eq}[CD_2Cl_2]$, where K_{eq} is defined as in the text. If the solvent concentration is assumed to be independent of temperature, the value of ΔH° is not affected, but the entropy term becomes $\Delta S^{\circ'} = \Delta S^\circ + R(\ln[CD_2Cl_2])$, where $R(\ln[CD_2Cl_2]) \approx 5.5$ eu.

(24) The dielectric constants (20 °C) are CH₂Cl₂ 9.08, C₆H₅Cl 5.71. *CRC Handbook of Chemistry and Physics*, 67th ed.; Weast, R. C., Astle, M. J., Beyer, W. H., Eds.; CRC Press: Boca Raton, FL, 1986; pp E-50–51.

(25) (a) Collins, S.; Koene, B. E.; Ramachandran, R.; Taylor, N. J. *Organometallics* **1991**, *10*, 2092. (b) Hong, Y.; Kuntz, B. A.; Collins, S. *Organometallics* **1993**, *12*, 964.

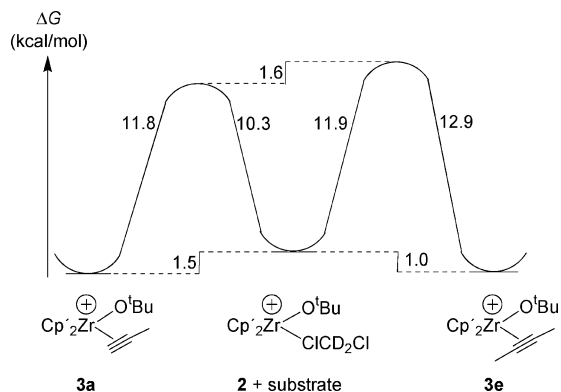


Figure 7. Free energy diagram ($-39\text{ }^{\circ}\text{C}$) comparing propyne and 2-butyne coordination to **2**.

(PMe_3) (**K**).²⁶ An X-ray crystallographic analysis of 1-hexyne adduct **J** revealed the presence of a symmetrically bound alkyne ligand ($d(\text{Zr}-\text{C}_{\text{int}}) = 2.211(3)\text{ \AA}$; $d(\text{Zr}-\text{C}_{\text{term}}) = 2.244(3)\text{ \AA}$; $\Delta d(\text{Zr}-\text{C}) = 0.033(4)\text{ \AA}$), with a $\text{C}\equiv\text{C}$ distance of $1.286(5)\text{ \AA}$ and a $\text{C}\equiv\text{C}-\text{C}$ angle of $135.8(3)^{\circ}$. The $\text{C}\equiv\text{C}$ NMR resonances of **J** and **K** are shifted far *downfield* from the free alkyne positions ($\Delta\delta = 60\text{--}120$), and the H_{term} resonance of **J** is also shifted significantly downfield upon coordination ($\Delta\delta \approx 5$). These results show that the alkyne ligands in **J** and **K** are symmetrically coordinated, the $\text{C}\equiv\text{C}$ bonds are not polarized, but the alkyne is strongly structurally distorted such that the “alkyne” carbons are sp^2 hybridized. The d^2 compounds $\text{Cp}^*_2\text{-Ti}(\text{MeC}\equiv\text{CMe})$,²⁷ $\text{Cp}^*_2\text{Ti}(\text{HC}\equiv\text{CMe})$,²⁸ $\text{Cp}_2\text{Nb}(\text{Et})(\text{HC}\equiv\text{CMe})$, and $\text{Cp}_2\text{Nb}(\text{H})(\text{HC}\equiv\text{CSiMe}_3)$ ²⁹ display similar properties. These effects are all characteristic of strong $\text{d}-\pi^*$ back-bonding, and these compounds are best described as d^0 metallocyclopropenes. In contrast, the absence of back-bonding in the d^0 metal–alkyne complexes **3a–g** results in weak unsymmetrical coordination, substantial polarization of the $\text{C}\equiv\text{C}$ bond, but little perturbation of the alkyne structure and hybridization of the alkyne carbons.³⁰ Other metal–alkyne complexes with weak or nonexistent $\text{d}-\pi^*$ back-bonding (e.g., **B**, **C**, **E**, **F**, **H**, and **I**; Charts 1 and 2) also show only minor coordination shifts and thus show a similar contrast to metal–alkyne complexes with back-bonding.

Comparison of d^0 Metal–Alkyne and d^0 Metal–Alkene Complexes. Alkynes bind more strongly to **2** than structurally similar alkenes do.¹⁴ For example, propyne binds to **2** almost 70 times stronger than propylene does, and propargyltrimethylsilane binds about 60 times stronger than allyltrimethylsilane does, based on the measured K_{eq} values. Steric effects probably contribute significantly to this difference, as the linear structure of alkynes creates less steric crowding with the $\text{Cp}'_2\text{Zr}$ backbone compared to alkenes. The ligand exchange behavior of alkyne and alkene complexes of **2** is quite similar. In both cases substrate decomplexation occurs by displacement by solvent in CD_2Cl_2 solution.

A free energy diagram comparing propylene and propyne coordination to **2** is shown in Figure 8. Propyne binds more strongly than propylene by ca. 1.7 kcal/mol. The barrier for

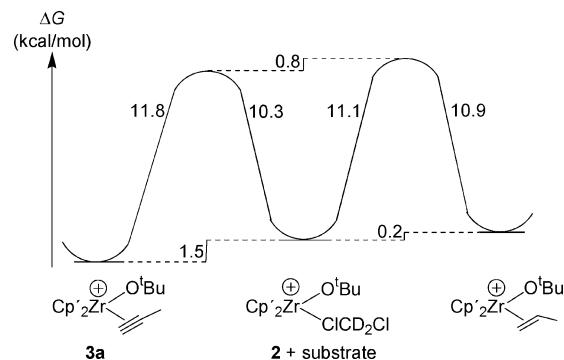


Figure 8. Free energy diagram ($-39\text{ }^{\circ}\text{C}$) comparing propyne and propylene coordination to **2**.

propyne decomplexation is higher than that for propylene decomplexation by ca. 0.9 kcal/mol, while the propyne complexation barrier is lower than that for propylene by ca. 0.8 kcal/mol. Thus, the stronger ligand propyne comes off more slowly, but binds more rapidly than the weaker ligand propylene.

Implications for Alkyne Oligomerization. Catalytic dimerization of terminal alkynes by Zr^{IV} compounds normally occurs via 1,2-alkyne insertion to give “head-to-tail” $\text{H}_2\text{C}=\text{CHRC}\equiv\text{CR}$ dimers as the major or exclusive product (Scheme 1). This selectivity implies that the $\text{Zr}-\text{C}\equiv\text{CR}$ group migrates to C_{int} of the coordinated alkyne.¹ Polarization of the $\text{C}\equiv\text{C}$ bond of the alkyne ligand in the key $\text{Cp}'_2\text{Zr}(\text{C}\equiv\text{CR})(\text{HC}\equiv\text{CR})^+$ intermediate in the same manner as implied by the NMR data for the $\text{Cp}'_2\text{Zr}(\text{O}^t\text{Bu})(\text{HC}\equiv\text{CR})^+$ models **3a–d** provides a reasonable explanation for this regiochemistry, as the partial positive charge on C_{int} of the alkyne renders this carbon susceptible to nucleophilic attack and thus insertion. It is also possible that steric crowding between the alkyl group of a terminal alkyne and the Cp ligands in the $\text{Cp}'_2\text{Zr}(\text{C}\equiv\text{CR})(\text{HC}\equiv\text{CR})^+$ intermediate would favor the alkyne rotamer in which C_{int} is oriented toward the $\text{M}-\text{R}$ bond, which would increase the preference for 1,2-alkyne insertion. The shielding of the O^tBu hydrogens of **3b** by the phenyl ring of the $\text{HC}\equiv\text{CPh}$ ligand suggests that such a rotamer is the favored one.

Experimental Section

General Procedures. All reactions were performed using glovebox or Schlenk techniques under a purified N_2 atmosphere or on a high-vacuum line. N_2 was purified by passage through columns of activated molecular sieves and Q-5 oxygen scavenger. CD_2Cl_2 and $\text{C}_6\text{D}_5\text{Cl}$ were distilled from P_2O_5 , while THF was distilled from Na/benzophenone. The synthesis of **2** was described previously.^{14a} Other reagents were obtained from standard commercial sources. $[\text{Ph}_3\text{C}][\text{B}(\text{C}_6\text{F}_5)_4]$ and propyne were used as received. Trimethylsilylacetylene and phenylacetylene were dried over CaH_2 . Propargyltrimethylsilane, 2-butyne, and 2-pentyne were dried over 3 Å molecular sieves. 3-Hexyne was dried over Na and stored over 3 Å molecular sieves prior to use.

NMR spectra were recorded on Bruker DRX 500 or 400 spectrometers in Teflon-valved NMR tubes at ambient probe temperature unless otherwise noted. ^1H and ^{13}C chemical shifts are reported relative to SiMe_4 and were referenced to the residual solvent signals. ^{19}F NMR spectra are reported and referenced relative to external neat CFCl_3 . NMR probe temperatures were calibrated by a MeOH thermometer.³¹ Coupling constants are reported in Hz. Where ^{13}C -gated- $\{^1\text{H}\}$ NMR spectra are reported, standard $^{13}\text{C}\{^1\text{H}\}$ NMR spectra were also recorded to assist in interpretation.

(26) Buchwald, S. L.; Watson, B. T.; Huffman, J. C. *J. Am. Chem. Soc.* **1987**, *109*, 2544.

(27) Cohen, S. A.; Bercaw, J. E. *Organometallics* **1985**, *4*, 1006.

(28) Brinkmann, P. H. P.; Luinstra, G. A.; Saenz, A. *J. Am. Chem. Soc.* **1998**, *120*, 2854.

(29) Yasuda, H.; Yamamoto, H.; Arai, T.; Nakamura, A.; Chen, J.; Kai, Y.; Kasai, N. *Organometallics* **1991**, *10*, 4058.

(30) Structural and vibrational spectroscopic data for Ti^{II} and Ti^{III} alkyne adducts substantiate the weakening of alkyne coordination upon loss of d electrons. Arndt, P.; Baumann, W.; Spannenberg, A.; Rosenthal, U.; Burlakov, V. V.; Shur, V. B. *Angew. Chem., Int. Ed.* **2003**, *42*, 1414.

(31) Van Geet, A. L. *Anal. Chem.* **1970**, *42*, 679.

NMR spectra of ionic compounds contain B(C₆F₅)₄⁻ anion resonances at the free anion positions, as listed in the Supporting Information. ¹⁹F NMR spectra were obtained for all compounds that contain this anion. NMR data for free alkynes are given in the Supporting Information.

General Procedure for Generation of [Cp'₂Zr(O^tBu)(alkyne)]-[B(C₆F₅)₄] (3a–g). An NMR tube was charged with **2** (25–50 mg), and CD₂Cl₂ (0.5–0.7 mL) was added by vacuum transfer at –78 °C. The tube was shaken at –78 °C, giving a yellow solution. The tube was cooled to –196 °C, and alkyne (excess) was added by vacuum transfer. The tube was warmed to –78 °C and shaken, yielding a yellow solution. The tube was placed in an NMR probe that had been precooled to –89 °C. NMR spectra were obtained and showed that a mixture of **3a–g**, **2**, and free alkene was present. The detailed procedure for propyne adduct **3a** and NMR data for all compounds are given below. The procedure for generation of **3b–g** is similar to that for **3a**.

Generation of [Cp'₂Zr(O^tBu)(HC≡CMe)][B(C₆F₅)₄] (3a). An NMR tube was charged with **2** (25.5 mg, 0.0255 mmol), and CD₂Cl₂ (0.70 mL) was added by vacuum transfer at –78 °C. The tube was shaken at –78 °C, giving a yellow solution. The tube was cooled to –196 °C, and propyne (0.0265 mmol) was added by vacuum transfer. The tube was warmed to –78 °C, shaken at –78 °C, and placed in an NMR probe that had been precooled to –89 °C. NMR spectra showed the presence of **3a** (0.026 M), **2** (0.0073 M), and free propyne (0.011 M). Raising the temperature from –89 °C has the effect of decreasing the concentration of **3a**, increasing the concentrations of **2** and free propyne, and broadening the signals for **3a** and to a lesser extent those of **2** and free propyne. As the temperature is raised, the signals for **3a** eventually coalesce with those of **2** and free propyne. Data for **3a**: ¹H NMR (CD₂Cl₂, –89 °C): δ 6.42 (m, 2H, Cp' CH), 6.37 (m, 2H, Cp' CH, overlaps with signal for **2**), 6.19 (m, 2H, Cp' CH), 6.06 (m, 2H, Cp' CH), 3.08 (q, *J* = 1.8, 1H, ≡CH), 2.23 (d, *J* = 1.5, 3H, ≡CMe), 2.17 (s, 6H, Cp' Me), 1.23 (s, 9H, O^tBu, overlaps with signal for **2**). ¹³C{¹H} NMR (CD₂Cl₂, –89 °C): δ 128.2 (ipso Cp'), 118.0 (Cp' CH), 116.1 (Cp' CH), 115.1 (Cp' CH), 110.5 (Cp' CH), 89.1 (d, ²*J*_{C=CH} = 47, C_{int}), 84.2 (OCMe₃), 64.2 (d, ¹*J*_{CH} = 251, C_{term}), 30.8 (OCMe₃), 14.8 (Cp' Me), 7.6 (q, ¹*J*_{CH} = 135, ≡CMe).

[Cp'₂Zr(O^tBu)(HC≡CPh)][B(C₆F₅)₄] (3b). ¹H NMR (CD₂Cl₂, –89 °C): δ 7.83 (d, *J* = 7.3, 2H, *o*-Ph), 7.78 (t, *J* = 7.3, 1H, *p*-Ph), 7.56 (t, *J* = 7.4, 2H, *m*-Ph), 6.34 (br s, 2H, Cp' CH, overlaps with signal for **2**), 6.30 (br s, 2H, Cp' CH), 6.09 (br s, 2H, Cp' CH), 6.06 (br s, 2H, Cp' CH), 4.46 (s, 1H, ≡CH), 2.22 (s, 6H, Cp' Me), 0.80 (s, 9H, O^tBu). ¹³C{¹H} NMR (CD₂Cl₂, –89 °C): δ 136.3 (*m*-Ph), 135.8 (*p*-Ph), 129.6 (*o*-Ph), 127.6 (ipso Cp'), 117.8 (Cp' CH), 115.7 (Cp' CH), 114.4 (Cp' CH), 110.9 (Cp' CH), 96.1 (d, ²*J*_{C=CH} = 41, C_{int}), 83.5 (OCMe₃), 75.0 (d, ¹*J*_{CH} = 246, C_{term}), 30.2 (OCMe₃), 15.0 (Cp' Me). The ipso-Ph resonance was not detected.

[Cp'₂Zr(O^tBu)(HC≡CSiMe₃)][B(C₆F₅)₄] (3c). ¹H NMR (CD₂Cl₂, –89 °C): δ 6.36 (br m, 2H, Cp' CH), 6.33 (br m, 2H, Cp' CH), 6.24 (br m, 2H, Cp' CH), 6.02 (br m, 2H, Cp' CH), 3.47 (s, 1H, CH), 2.14 (s, 6H, Cp' Me), 1.24 (s, 9H, O^tBu), 0.44 (s, 9H, SiMe₃). ¹³C{¹H-gated} NMR (CD₂Cl₂, –89 °C): δ 126.9 (s, ipso Cp'), 118.3 (d, ¹*J*_{CH} = 177, Cp' CH), 117.1 (d, ¹*J*_{CH} = 170, Cp' CH), 114.7 (d, ¹*J*_{CH} = 177, Cp' CH), 109.5 (d, ¹*J*_{CH} = 179, Cp' CH), 94.3 (C_{int}),³² 90.1 (d, ¹*J*_{CH} = 244, C_{term}), 84.8 (s, OCMe₃), 30.9 (q, ¹*J*_{CH} = 125, OCMe₃), 14.8 (q, ¹*J*_{CH} = 129, Cp' Me), –0.5 (q, ¹*J*_{CH} = 122, SiMe₃).

[Cp'₂Zr(O^tBu)(HC≡CCH₂SiMe₃)][B(C₆F₅)₄] (3d). ¹H NMR (CD₂Cl₂, –89 °C): δ 6.33 (br m, 2H, Cp' CH), 6.31 (br s, 2H, Cp' CH), 6.13 (br m, 2H, Cp' CH), 5.99 (br m, 2H, Cp' CH), 3.46 (br s, 1H, ≡CH), 2.13 (s, 6H, Cp' Me), 1.91 (br s, 2H, CH₂SiMe₃),

1.19 (s, 9H, O^tBu), 0.21 (s, 9H, SiMe₃). ¹³C-gated-{¹H} NMR (CD₂Cl₂, –89 °C): δ 127.5 (s, ipso Cp'), 117.4 (d, ¹*J*_{CH} = 169, Cp' CH), 115.6 (d, ¹*J*_{CH} = 171, Cp' CH), 114.5 (d, ¹*J*_{CH} = 174, Cp' CH), 110.1 (d, ¹*J*_{CH} = 173, Cp' CH), 104.3 (d, ²*J*_{C=CH} = 43, C_{int}), 83.4 (s, OCMe₃), 65.5 (d, ¹*J*_{CH} = 244, C_{term}), 30.8 (q, ¹*J*_{CH} = 126, OCMe₃), 14.8 (q, ¹*J*_{CH} = 129, Cp' Me), 12.7 (t, ¹*J*_{CH} = 131, CH₂SiMe₃), –2.6 (q, ¹*J*_{CH} = 121, SiMe₃).

[Cp'₂Zr(O^tBu)(MeC≡CMe)][B(C₆F₅)₄] (3e). ¹H NMR (C₆D₅-Cl, –35 °C): δ 5.95 (br s, 2H, Cp' CH), 5.61 (br s, 2H, Cp' CH), 1.92 (s, 6H, Cp' Me), 1.55 (s, 6H, MeC≡CMe), 0.97 (s, 9H, O^tBu). The other Cp' CH resonances are obscured by signals for **2**. ¹H NMR (CD₂Cl₂, –89 °C): δ 6.33 (br s, 2H, Cp' CH, overlaps with signal for **2**), 6.30 (br s, 2H, Cp' CH), 6.23 (br s, 2H, Cp' CH), 6.00 (br s, 2H, Cp' CH), 2.23 (s, 6H, Cp' Me), 2.03 (br s, 6H, MeC≡CMe), 1.23 (s, 9H, O^tBu, overlaps with signal for **2**). ¹³C{¹H} NMR (C₆D₅-Cl, –35 °C): δ 118.1 (Cp' CH), 116.4 (Cp' CH), 114.4 (Cp' CH), 111.5 (Cp' CH), 84.4 (OCMe₃), 80.0 (C≡C), 31.2 (OCMe₃), 14.3 (Cp' Me), 8.8 (MeC≡CMe). The ipso Cp' resonance is obscured by a solvent resonance. ¹³C{¹H} NMR (CD₂Cl₂, –89 °C): δ 128.5 (ipso Cp'), 118.2 (Cp' CH), 116.1 (Cp' CH), 113.7 (Cp' CH), 110.7 (Cp' CH), 84.3 (OCMe₃), 79.6 (C≡C), 31.1 (OCMe₃), 14.5 (Cp' Me), 9.7 (br, MeC≡CMe).

[Cp'₂Zr(O^tBu)(MeC≡CEt)][B(C₆F₅)₄] (3f). ¹H NMR (CD₂Cl₂, –89 °C): δ 6.35 (br s, 2H, Cp' CH), 6.29 (br s, 2H, Cp' CH), 6.23 (br m, 2H, Cp' CH), 6.00 (br s, 2H, Cp' CH), 2.23 (s, 6H, Cp' Me), 2.06 (unresolved m, 3H, ≡CMe, partially overlaps with a resonance for free 2-pentyne), 1.27 (br t, *J* = 8, 3H, CH₂Me, partially obscured by O^tBu resonances of **3f** and **2**), 1.23 (s, 9H, O^tBu, overlaps with resonance for **2**). The ≡CCH₂ signal is obscured by the Cp' Me signal for **2**. ¹³C{¹H-gated} NMR (CD₂Cl₂, –89 °C): δ 128.3 (s, ipso Cp'), 118.2 (d, ¹*J*_{CH} = 177, Cp' CH), 116.0 (d, ¹*J*_{CH} = 171, Cp' CH), 113.8 (d, ¹*J*_{CH} = 174, Cp' CH), 110.7 (d, ¹*J*_{CH} = 174, Cp' CH), 84.3 (s, OCMe₃), 84.0 (slightly br s, C≡C), 81.6 (slightly br s, C≡C), 31.1 (q, ¹*J*_{CH} = 126, OCMe₃), 19.0 (br t, ¹*J*_{CH} = 135, ≡CCH₂), 14.6 (q, ¹*J*_{CH} = 128, Cp' Me), 14.5 (partially obscured br q, CH₂Me), 9.9 (br q, ¹*J*_{CH} = 134, MeC≡).

[Cp'₂Zr(O^tBu)(EtC≡CEt)][B(C₆F₅)₄] (3g). ¹H NMR (CD₂Cl₂, –89 °C): δ 6.33 (br m, 2H, Cp' CH), 6.28 (br m, 2H, Cp' CH), 6.20 (br m, 2H, Cp' CH), 5.98 (br m, 2H, Cp' CH), 2.22 (s, 6H, Cp' Me), 1.29 (br t, *J* = 7, 6H, MeCH₂C≡), 1.22 (s, 9H, O^tBu, overlaps with O^tBu signal of **2**). The MeCH₂C≡ signal is obscured by the Cp' Me signal of **3g** and **2**. ¹³C{¹H-gated} NMR (CD₂Cl₂, –89 °C): δ 128.2 (s, ipso Cp'), 118.1 (d, ¹*J*_{CH} = 172, Cp' CH), 115.8 (d, ¹*J*_{CH} = 171, Cp' CH), 113.8 (d, ¹*J*_{CH} = 172.4, Cp' CH), 110.6 (d, ¹*J*_{CH} = 181, Cp' CH), 86.5 (s, C≡C), 84.3 (s, OCMe₃), 31.1 (q, ¹*J*_{CH} = 127, OCMe₃), 19.0 (br t, ¹*J*_{CH} = 135, CH₂C≡), 14.6 (MeCH₂C≡),³³ 14.6 (q, ¹*J*_{CH} = 128, Cp' Me).

Competitive Coordination of Propyne and THF to 2. A solution of **2** (0.0270 mmol) in CD₂Cl₂ (0.71 mL) in an NMR tube was generated as described above. The tube was cooled to –196 °C, and THF (0.0292 mmol, 1.08 equiv) was added by vacuum transfer. The tube was warmed to –78 °C and shaken to give a yellow solution. The tube was cooled to –196 °C, and propyne (0.41 mmol, 15 equiv) was added by vacuum transfer. The tube was warmed to –78 °C, shaken to give a yellow solution, and then placed in a precooled NMR probe. NMR spectra recorded at –89 and –38 °C revealed the presence of [Cp'₂Zr(O^tBu)(THF)]-[B(C₆F₅)₄] (**4**; 100%), along with free THF (0.097 equiv) and free propyne (15 equiv). [Cp'₂Zr(O^tBu)(HC≡CMe)][B(C₆F₅)₄] (**3a**) was not observed.

Independent Generation of [Cp'₂Zr(O^tBu)(THF)][B(C₆F₅)₄] (4). A solution of **2** (0.0701 mmol) in C₆D₅-Cl (0.6 mL) was cooled to –196 °C, and THF (0.0717 mmol, 1.02 equiv) was added by vacuum transfer. The tube was warmed to 22 °C and shaken to give a yellow-orange solution. NMR spectra showed that **4** had formed quantitatively. Data for **4**: ¹H NMR (C₆D₅-Cl): δ 5.94–5.91 (m, 4H, Cp' CH), 5.79 (q, *J* = 2.5, 2H, Cp' CH), 5.73 (q, *J* =

(32) While the resonance is clear in the ¹³C{¹H} NMR spectrum, the coupling pattern in the ¹³C{gated-¹H} spectrum is obscured by a free alkyne resonance.

2.9, 2H, Cp' CH), 3.51 (m, 4H, THF), 1.85 (s, 6H, Cp'Me), 1.65 (m, 4H, THF), 1.01 (s, 9H, O'Bu). ¹H NMR (CD₂Cl₂, -89 °C): δ 6.36 (br s, 2H, Cp' CH), 6.31 (br s, 2H, Cp' CH), 6.15 (br s, 2H, Cp' CH), 6.07 (br s, 2H, Cp' CH), 3.96 (br m, 4H, THF), 2.13 (s, 6H, Cp'Me), 2.10 (br m, 4H, THF), 1.21 (s, 9H, O'Bu). ¹³C{¹H} NMR (C₆D₅Cl): δ 127.6 (ipso Cp'), 117.6 (Cp' CH), 116.2 (Cp' CH), 115.3 (Cp' CH), 111.2 (Cp' CH), 78.0 (THF), 31.6 (OCMe₃), 25.7 (THF), 14.4 (Cp'Me); the OCMe₃ resonance was not detected. ¹³C{¹H} NMR (CD₂Cl₂, -89 °C): δ 126.9 (ipso Cp'), 117.0 (Cp' CH), 115.0 (Cp' CH), 114.9 (Cp' CH), 109.9 (Cp' CH), 82.3 (OCMe₃), 78.0 (THF), 31.0 (OCMe₃), 25.7 (THF), 14.3 (Cp'Me).

Influence of [Ph₃C][B(C₆F₅)₄] on 2-Butyne Coordination to 2. An NMR tube was charged with **2** (19.3 mg, 0.0193 mmol) and [Ph₃C][B(C₆F₅)₄] (48.9 mg, 0.0530 mmol, 2.75 equiv), and CD₂-Cl₂ (0.71 mL) was added by vacuum transfer at -78 °C. The tube was shaken at -78 °C to give a deep yellow solution and then cooled to -196 °C. 2-Butyne (0.0241 mmol, 1.25 equiv) was added by vacuum transfer. The tube was warmed to -78 °C, shaken, and placed in an NMR probe that had been precooled to -91 °C. NMR spectra showed that **3e** (0.015 M), **2** (0.013 M), free 2-butyne (0.028 M), and Ph₃C⁺ (0.084 M) were present. The B(C₆F₅)₄⁻ concentration was 0.11 M (sum of [**3e**] + [**2**] + [Ph₃C⁺]). The equilibrium constant, $K_{eq} = [\mathbf{3e}][\mathbf{2}]^{-1}[\text{MeC}\equiv\text{CMe}]^{-1} = 41(9) \text{ M}^{-1}$, agrees with the value found without added [Ph₃C][B(C₆F₅)₄] (52(3) M⁻¹). ¹H, ¹⁹F, and ¹³C NMR spectra of a CD₂Cl₂ solution containing [Ph₃C]-[B(C₆F₅)₄] (0.042 M) and 2-butyne (0.037 M) showed that there is no detectable interaction between these species at -86 °C.

Competitive Coordination of Propargyltrimethylsilane and Propyne to 2. A solution of **2** (0.0206 mmol) in CD₂Cl₂ (0.63 mL) was generated as described above. The tube was cooled to -196 °C, and propargyltrimethylsilane (0.026 mmol) was added by vacuum transfer. The tube was warmed to -78 °C and shaken, yielding a yellow solution. The tube was cooled to -196 °C, and propyne (0.085 mmol) was added by vacuum transfer. The tube was warmed to -78 °C and shaken, yielding a yellow solution. The tube was placed in an NMR probe that had been precooled to -89 °C. NMR spectra showed that a mixture of [Cp'Zr(O'Bu)(HC≡CCH₂SiMe₃)] [B(C₆F₅)₄] (**3d**, 0.032 M), [Cp'Zr(O'Bu)(HC≡CMe)] [B(C₆F₅)₄] (**3a**; 0.0017 M), free propargyltrimethylsilane (0.0089 M), and free propyne (0.13 M) was present. **2** was not present. This equilibrium was studied in three experiments, in which the initial concentrations were [**2**]_{initial} = 0.033(1) M, [HC≡CMe]_{initial} = 0.14–0.26 M, and [HC≡CCH₂SiMe₃]_{initial} = 0.040–0.089 M, and the order of alkyne addition was reversed in one experiment.

Reaction of 2 with *tert*-Butylacetylene. An NMR tube was charged with **2**, and CD₂Cl₂ (ca. 0.60 mL) was added by vacuum transfer at -78 °C. The tube was shaken at this temperature, giving a yellow solution. The tube was cooled to -196 °C, and excess *tert*-butylacetylene was added by vacuum transfer. The tube was warmed to -78 °C, shaken, and placed in an NMR probe cooled to -89 °C. NMR spectra showed that mixtures of **2** and free *tert*-butylacetylene were present. No resonances or line broadening effects indicative of ligand coordination to **2** were observed.

Determination of Thermodynamic Parameters and Exchange Rates. (A) General Variable-Temperature NMR Procedure. NMR samples were prepared as described above. The NMR tube was stored at -78 °C and placed in a precooled NMR probe. The probe was maintained at a given temperature for 20–30 min to allow the sample to reach thermal equilibrium, and then NMR experiments were conducted. The temperature was raised 5 or 10 °C and the procedure repeated until the desired temperature range had been studied.

(B) Equilibrium Constant Measurements. Equilibrium constants for eq 1, $K_{eq} = [\mathbf{3}][\mathbf{2}]^{-1}[\text{alkyne}]^{-1}$, were determined by multiple (typically 2–4) ¹H NMR experiments in which [**2**]_{initial}

and [alkyne]_{initial} were varied. For **3a–c,e–g**, K_{eq} values were determined by direct study of the equilibria in eq 1.

For the equilibrium involving **3a**, the relative amounts of **3a**, **2**, and free propyne were determined from the integrals of the H_{term} resonance of **3a**, the O'Bu resonance of **2** after the contribution from **3a** was subtracted, and both free propyne resonances. The number of moles of **3a** and **2** was determined by finding their respective mole fractions and multiplying by the original amount of **2** used. The number of moles of free propyne was determined from the ratio of the integrals of the free and coordinated propyne resonances. Concentrations were determined by dividing the number of moles by the solution volume. K_{eq} values for **3a** were measured between -89 and -8 °C.

The methodology for determining the K_{eq} values for **3b–c,e–g** was similar. Calculations of molar amounts and K_{eq} values for **3b–g** were determined as described for **3a**. K_{eq} values for **3b–d,f,g** were measured at -89 °C. K_{eq} values for **3e** were measured between -89 and -3 °C. The choices for integrals for the relative amounts involving **3b,c,e–g** are given below.

For the equilibrium involving **3b**, relative amounts of **3b**, **2**, and free phenylacetylene were determined from the integrations of the H_{term} signal of **3b**, the Cp'Me and O'Bu resonance after the contribution from **3b** was subtracted for **2**, and the H_{term} resonance for free phenylacetylene.

For the equilibrium involving **3c**, relative amounts of **3c**, **2**, and free trimethylsilylacetylene were determined from the integrations of the SiMe₃ resonance of **3c**, the O'Bu resonance after the contribution from **3c** was subtracted for **2**, and the H_{term} resonance of free trimethylsilylacetylene.

For the equilibrium involving **3e**, relative amounts of **3e**, **2**, and free 2-butyne were determined from the integrations for coordinated 2-butyne, the O'Bu resonance after the contribution from **3e** was subtracted for **2**, and the free 2-butyne resonance. K_{eq} values were found between -89 and -3 °C.

For the equilibrium involving **3f**, relative amounts of **3f**, **2**, and free 2-pentyne were determined from the most upfield Cp' CH resonance of **3f**, the O'Bu resonance after the contribution from **3f** was subtracted for **2**, and both Me resonances of free 2-pentyne.

For the equilibrium involving **3g** relative amounts of **3g**, **2**, and free 2-hexyne were determined from the two most upfield Cp' CH resonances of **3g**, the Cp'Me resonance after the contribution from **3g** was subtracted for **2**, and the Me resonance for free 3-hexyne.

The K_{eq} value for formation of propargyltrimethylsilane adduct **3d** in eq 1, $K_{eq,3d} = [\mathbf{3d}][\mathbf{2}]^{-1}[\text{HC}\equiv\text{CCH}_2\text{SiMe}_3]^{-1}$, was determined by competition experiments with propyne in CD₂Cl₂ solution at -89 °C. The equilibrium constant for the reaction



was defined to be $K_1 = [\mathbf{3d}][\text{propyne}][\mathbf{3a}]^{-1}[\text{HC}\equiv\text{CCH}_2\text{SiMe}_3]^{-1}$ and was determined by ¹H NMR studies of this equilibrium. The relative concentrations of **3d**, **3a**, free propargyltrimethylsilane, and free propyne were found from the integrals of the H_{term} resonance of **3d**, the H_{term} resonance of **3a**, the CH₂ and SiMe₃ resonances of free propargyltrimethylsilane, and the Me resonance of free propyne. The equilibrium constant for propyne coordination to **2** to form **3a** is $K_{eq,3a} = [\mathbf{3a}][\mathbf{2}]^{-1}[\text{HC}\equiv\text{CMe}]^{-1}$ and was determined as described above. $K_{eq,3d}$ is given by $K_{eq,3d} = K_1 K_{eq,3a}$.

Thermodynamic parameters (ΔH° and ΔS°) were determined from van't Hoff plots of ln(K_{eq}) versus 1/T for each variable-temperature NMR run. The reported values are the weighted average of results from at least three runs in which the initial concentrations of **2** and alkyne were varied.³⁴

(33) While the resonance is clear in the ¹³C{¹H} NMR spectrum, the coupling pattern in the ¹³C{gated-¹H} spectrum is obscured by the Cp'Me resonance of **3g**.

(C) Exchange Rate Measurements. Rate constants for alkyne decomplexation (k_{-1}) for **3a** and **3e** were determined by variable-temperature ¹H NMR spectroscopy. For **3a**, the rate of propyne decomplexation was determined from the line shape of the ≡CH resonance of coordinated propyne by fitting simulated spectra to experimental spectra using gNMR to perform an iterative full line shape analysis.³⁵ The line width at half-height of the benzene resonance (ω_0) was used as the line width in the absence of exchange. The ⁴J_{HH} value for propyne was set at 1.8 Hz and assumed to be temperature-independent. The rate values were converted to first-order rate constants k_{-1} by the formula $\text{rate} = k_{-1}[\mathbf{3a}]$. Measurements were made over a temperature range of -69 to +22 °C.

For **3e**, rate constants for 2-butyne decomplexation were determined from the line widths of the coordinated 2-butyne resonance. The line width at half-height of the benzene resonance was used as the line width in the absence of exchange (ω_0) for coordinated 2-butyne at each temperature. First-order rate constants

(34) The weighted average \bar{x} is defined as $(\sum w_i x_i)/(\sum w_i)$ and the weighted standard deviation (σ) is defined by $\sigma^2 = \{\sum w_i (x_i - \bar{x})^2\}/\{\sum w_i\}$, where the weighing factors are $w_i = 1/\sigma_i^2$.

(35) gNMR, v. 4.1.2; Adept Scientific: Letchworth, UK, 2000.

for 2-butyne decomplexation (k_{-1}) were determined by the formula $k_{-1} = \pi(\omega - \omega_0)$, where ω is the line width at half-height of the coordinated 2-butyne resonance. All measurements were made in the slow exchange region between -48 and -8 °C.

For **3a,e**, k_{-1} values were determined in at least three experiments with different initial concentrations of **2** and alkyne. The k_{-1} values were found to be independent of the concentrations of **2**, free alkyne, and **3a** or **3e**, consistent with the rate law $\text{rate} = k_{-1}[\mathbf{3}]$. Activation parameters for decomplexation were determined from Eyring plots of $\ln(k_{-1}/T)$ versus $1/T$. The reported values are the weighted averages of results from at least three runs.³⁴

Acknowledgment. We thank the NSF (CHE-0212210) for financial support and the University of Chicago for a William Rainey Harper fellowship (E.J.S.).

Supporting Information Available: NMR data for free alkynes (pdf). This material is available free of charge via the Internet at <http://pubs.acs.org>.

OM050947F